NIH RELAIS Document Delivery

NIH-10286759

JEFFDUYN

NIH -- W1 AN6151

JOZEF DUYN
10 Center Dirve
Bldg. 10/Rm.1L07
Bethesda, MD 20892-1150

ATTN:
PHONE: 301-594-7305
FAX: -
E-MAIL:

SUBMITTED: 2002-08-29 17:22:17
PRINTED: 2002-08-31 12:18:36
REQUEST NO.:NIH-10286759
SENT VIA: LOAN DOC
7967421

NIH Fiche to Paper Journal

TITLE: ANNALS OF NEUROLOGY
PUBLISHER/PLACE: Wiley-Liss New York, NY :
VOLUME/ISSUE/PAGES:1994 Oct;36(4):595-608 595-608
DATE: 1994
AUTHOR OF ARTICLE: Kruse B; Barker PB; van Zijl PC; Duyn JH; Moonen CT; Moser H
TITLE OF ARTICLE: Multislice proton magnetic resonance spectroscopic
ISSN: 0364-5134
OTHER NOS/LETTERS: Library reports holding volume or year
7707449
7944292
SOURCE: PubMed
CALL NUMBER: W1 AN6151
REQUESTER INFO: JEFFDUYN
DELIVERY: E-mail: jhd@helix.nih.gov
REPLY: Mail:

Multislice Proton Magnetic Resonance Spectroscopic Imaging in X-linked Adrenoleukodystrophy

Bernd Kruse, MD,* Peter B. Barker, DPhil,† Peter C. M. van Zijl, PhD,† Jeff H. Duyn, PhD,‡ Chrit T. W. Moonen, PhD,‡ and Hugo W. Moser, MD*

Multislice proton magnetic resonance spectroscopic imaging permits metabolic analysis of brain tissue in vivo by data acquisition in four oblique axial slices, each 15-mm thick and divided into 0.8-ml single-volume elements. We applied this technique to the systematic study of 25 patients with adrenoleukodystrophy: 3 with the severe childhood or adult cerebral form of the disease, 5 with adrenomyeloneuropathy, 12 with no demonstrable neurological involvement, and 5 women heterozygous for adrenoleukodystrophy who had some degree of neurological disability. Abnormalities on magnetic resonance spectroscopic imaging included a reduction in *N*-acetyl aspartate, an increase in choline-containing compounds, and at times, an increase in lactate. Five patients showed abnormalities in the presence of normal-appearing magnetic resonance images, and in 8 other patients the alterations on spectroscopic images were more severe than those demonstrable by magnetic resonance imaging. Correlation with clinical course suggests that an increase in the choline-containing compounds is associated with an active demyelinative process, whereas such compounds are not elevated in lesions that are stable. We conclude that magnetic resonance spectroscopic imaging is a more sensitive indicator of early neurological involvement than is magnetic resonance imaging, and that the character of abnormalities detected by the former technique may serve as a gauge of the degree of activity of the demyelinating process and as a guide to the selection and evaluation of therapeutic approaches.

Kruse B, Barker PB, van Zijl PCM, Duyn JH, Moonen CTW, Moser HW. Multislice proton magnetic resonance spectroscopic imaging in X-linked adrenoleukodystrophy. Ann Neurol 1994;36:595–608

X-linked adrenoleukodystrophy (ALD) is a genetically determined disorder that involves mainly nervous system white matter, adrenal cortex, and testis [1]. It is associated with the abnormal accumulation of saturated very-long-chain fatty acids (VLCFAs) in tissues [2], plasma [3], and red blood cells [4] due to an impaired capacity to degrade them [5]. The putative gene defect was identified recently. The gene maps to Xq28, the terminal segment of the long arm of the X chromosome [6], and codes for a peroxisomal membrane protein [7].

The phenotypic expression of ALD varies widely. The childhood cerebral form (cALD), which manifests most commonly between ages 4 and 8 years and often progresses to an apparently vegetative state within 2 years [8], is the most common phenotype and appears in about 50% of ALD patients [9]. The next most common phenotype, affecting about 25% of ALD patients, is adrenomyeloneuropathy (AMN), which manifests in early adulthood, mainly involves the spinal cord and peripheral nerves, and progresses over decades [10]. About 20% of patients have adrenal involvement only (Addison's disease) or are asymptomatic. The adolescent and adult cerebral types (aALD) occur in 5 and 3% of patients, respectively. In about 20% of women heterozygous for ALD, neurological disabilities that resemble those in AMN develop [11].

Phenotype assignment has important implications for prognosis, counseling, and the selection of therapeutic approaches. For instance, at the present time bone marrow transplantation (BMT) is recommended *only* for children with evidence of *early* cerebral involvement [9, 12]. It is not recommended for children with advanced disease, because the procedure not only is ineffective, but may even accelerate the rate of progression of the neurological handicap [9, 13]. Conversely, BMT is not indicated for patients who are *free* of demonstrable cerebral involvement, because these patients may be "destined" for the milder adult phenotypes, and it would not be ethically justifiable to subject them to the risk of BMT. Therefore, it is of practical importance to distinguish as accurately as possible

From the *Kennedy Krieger Institute, Baltimore; †Department of Radiology, Johns Hopkins University School of Medicine, Baltimore; and ‡Laboratory of Diagnostic Radiology Research, National Institutes of Health, Bethesda, MD.

Received Dec 27, 1993, and in revised form Feb 28, 1994. Accepted for publication Mar 31.

Address correspondence to Dr Moser, Kennedy Krieger Institute, 707 North Broadway, Baltimore, MD 21205.

patients who have mild and early cerebral involvement from those who have none, and also to grade the severity of cerebral involvement so that invasive therapies are not offered when the disease has advanced too far. In particular, for the neurologically asymptomatic ALD patients, it is important to take advantage of a "window of opportunity" for invasive therapies such as BMT. Consequently, we monitor asymptomatic patients at 6- to 12-month intervals during the age at which they are at greatest risk for cALD. This monitoring process includes neurological examination, magnetic resonance imaging (MRI), and detailed tests of cognitive function [14]. Nevertheless, determining the presence or absence of cerebral involvement has been difficult for patients who show early cognitive defects but an apparently normal MRI, and in patients who show equivocal white matter signal increases on T2-weighted images.

During the past year we combined MRI with the newly developed multislice proton magnetic resonance spectroscopic imaging (MRSI) technique [15]. This method allows an in vivo metabolic analysis of four brain slices (thickness, 15 mm), which are divided into planar volume elements (voxels) with a size of 0.8 ml. Metabolites detectable with this method include *N*-acetyl aspartate (NAA), choline-containing compounds (Cho), creatine and phosphocreatine (Cr), and lactate (Lac). To our knowledge, this report represents the first clinical application of this new technique. The data presented here indicate that MRSI permits earlier detection of cerebral involvement than is possible by MRI, and also increases the capacity to evaluate the significance and rate of progression of abnormal MRI findings.

Patients and Methods

Patient Population

All patients were participants in a trial of dietary therapy of ALD conducted at the Kennedy Krieger Institute and the Johns Hopkins Hospital. We selected 25 patients who encompassed the full range of ALD phenotypes and compared their results with those in 12 healthy control subjects (9 males and 3 females; mean age, 37 years; range, 5–74 years). Table 1 summarizes clinical data, including sex, age at examination, disease phenotype, information about dietary therapy, adrenal function, and an overview of MRI and MRSI results.

Two patients had the childhood cerebral type of the disease and 1 patient had the adult cerebral form. Five patients were classified as AMN and 12 patients as asymptomatic. Five heterozygote women, including a pair of twins, were included. Age at examination ranged from 30 months (Patient 12) to 70 years (Patients 24 and 25), with a mean of 48 years.

Neurological symptoms ranged from the characteristic severe cerebral involvement with spastic paresis, mental, visual, and hearing impairments and a rapidly progressive course to a vegetative state in the patients with cALD, to normal findings in asymptomatic patients. Between these two extremes patients belonging to different phenotypes showed different degrees of neurological involvement.

Adrenal insufficiency was present and treated with hormone supplementation in 16 patients. Adrenal function was normal in the other 9 patients, including the 2 youngest patients and the 5 women.

Because of the advanced stage of his illness, Patient 1 did not receive the dietary therapy with glyceryl trioleate and glyceryl trierucate, also referred to as "Lorenzo's oil"; Patients 7 and 9 had stopped the diet; and Patient 8 did not take the oil on a regular basis. Seven patients (Patients 6, 10, 12, 21, 22, 24, and 25) had been on dietary therapy less than 1 month at the time of the MRSI examination and were classified as "prediet." The remaining 14 patients were treated with Lorenzo's oil for at least 1 month and participated in regular (once a year) follow-up examinations, including neurological, neuropsychological, biochemical, cardiological, neurophysiological, and neuroradiological tests.

The study was approved by the Joint Committee on Clinical Investigation at the Johns Hopkins University School of Medicine.

MRI and MRSI Procedures

Magnetic resonance examinations in all patients were performed using a 1.5-T whole-body system (Signa; GE Medical Systems, Milwaukee, WI). Prior to the MRSI examination, sagittal T1-weighted (repetition time [TR] 500 msec/echo time [TE] 20 msec; thickness, 5 mm) and axial double-echo MRIs (TR 3000/TE 30/100; thickness, 5 mm) were obtained from all patients. Patients who were unable to cooperate were sedated with chloral hydrate (50–100 mg/kg of body weight). Physiological indices were checked during the investigation by pulse oximetry. MRIs were evaluated independently by an attending neuroradiologist and one of us (B. K.). For the purpose of this study, MRIs were classified as either normal, abnormal (changes of signal intensities in white matter due to leukodystrophy, signs of atrophy), or abnormal-MN (changes either very mild or not ALD related).

Four oblique-axial slices (nominal thickness, 15 mm; intersectional gap, 2.5 mm) parallel to the anterior commissure–posterior commissure line were selected for the MRSI examination. Outer volume saturation pulses were used for suppression of lipid and water signals originating from the skull and scalp, and a chemical shift-selective saturation pulse for water suppression. The four slices were recorded interleaved with a TR of 2300 msec and a TE of 272 msec, giving a total of 30 minutes for data acquisition. Technical details are given elsewhere [15–17].

Data processing of each individual slice was performed independently on a Sun workstation (Sun Microsystems, Mountain View, CA) by two investigators (B. K., P. B. B.). Spectroscopic images for NAA at 2.02 ppm, Cho at 3.24 ppm, Cr at 3.03 ppm, and Lac at 1.33 ppm were created for each slice by integration of peak areas. Each slice was divided in 32 × 32 voxels, with a nominal voxel size of 0.8 ml. Cosine filtering was applied in the k-space domains, giving an effective voxel size approximately double the nominal size. Sometimes a "ringing" artifact from the residual water signal was seen in the spectra; this resulted from truncation of the time-domain signals. Spectra were evaluated in voxels located

Table 1. Clinical Data from 25 Patients with Adrenoleukodystrophy[a]

Patient No.	Sex	Age (yr;mo)	Phenotype	Diet	Addison	MRI	MRSI
1	M	5;11	cALD	No	Yes	Abnormal	More widespread
2	M	13	cALD	Yes	Yes	Abnormal	Equivalent
3	M	29;4	aALD	Yes	Yes	Abnormal	More widespread
4	M	29;4	AMN	Yes	Yes	Abnormal-MN	More widespread
5	M	57;5	AMN	Yes	Yes	Normal	Equivalent
6	M	22;9	AMN	Pre	No	Normal	Abnormal
7	M	36;5	AMN	Off	Yes	Abnormal	More widespread
8	M	36;5	AMN	Yes-N	Yes	Abnormal	More widespread
9	M	22;7	Asympt.	Off	No	Normal	Equivalent
10	M	5;9	Asympt.	Pre	No	Normal	Abnormal
11	M	15;7	Asympt.	Yes	Yes	Normal	Abnormal
12	M	2;6	Asympt.	Pre	No	Abnormal	More widespread
13	M	11;6	Asympt.	Yes	Yes	Normal	Equivalent
14	M	9;3	Asympt.	Yes	Yes	Abnormal	Equivalent
15	M	13;4	Asympt.	Yes	Yes	Normal	Abnormal
16	M	9;9	Asympt.	Yes	Yes	Normal	Equivalent
17	M	9;6	Asympt.	Yes	Yes	Normal	Equivalent
18	M	10;10	Asympt.	Yes	Yes	Abnormal	Equivalent
19	M	16;9	Asympt.	Yes	Yes	Abnormal-MN	More widespread
20	M	15;6	Asympt.	Yes	Yes	Abnormal	Equivalent
21	F	49	Heteroz.	Pre	No	Abnormal	Equivalent
22	F	55;9	Heteroz.	Pre	No	Normal	Abnormal
23	F	47;11	Heteroz.	Yes	No	Normal	Equivalent
24	F	70	Heteroz.	Pre	No	Abnormal-MN	More widespread
25	F	70	Heteroz.	Pre	No	Abnormal-MN	Normal

[a]The patients are grouped into different phenotypes: childhood cerebral type (cALD), adolescent or adult cerebral type (aALD), adrenomyeloneuropathy (AMN), asymptomatic (Asympt.), and symptomatic heterozygote women (Heteroz.). Sex, age at examination, status of the dietary therapy (pre = prediet; yes-N = noncompliant), and information about the adrenal function are given, as well as a comparison of the MRSI results to the recent MRI findings. The MRI findings were graded into normal, abnormal, or abnormal-MN (abnormalities mild or not ALD related).

MRI = magnetic resonance imaging; MRSI = magnetic resonance spectroscopic imaging.

in parietooccipital paramedian gray matter, and periventricular frontal and periventricular occipital white matter, in corresponding positions in all patients and in all control subjects. The top and the bottom slices contained mainly gray matter regions (cortex and basal ganglia, respectively) and were not chosen for spectral evaluation for this study. With respect to white matter changes seen on MRI, an additional subdivision into so-called "affected" and "unaffected" areas of white matter was made. For more objective information we evaluated two spectra in the neighboring middle slices in each of the above-mentioned regions. In some patients, however, spectra in indicated locations were not suitable for a detailed evaluation owing to poor technical quality caused by patient movement or susceptibility artifacts. These regions are referred to as "not determined" (ND) in Table 2.

Quantitative metabolite measurements were made by integration of the peak areas in selected brain locations in both gray and white matter. Metabolite ratios were considered "abnormal" if they were more than 2 standard deviations different from control values (see Table 2). Since a relatively constant distribution of Cr was observed throughout the brain in most patients, the metabolite integrals are expressed as ratios of NAA to Cr, and Cho to Cr, respectively. Assuming an absolute Cr concentration of about 5 to 9 μmol/gm of wet weight in human brain tissue in vivo [18, 19], the concentration of NAA and Cho can be estimated from the ratios. Since a mild decrease of NAA was often combined with a mild increase of Cho, the NAA/Cho ratio was also calculated and this facilitated detection of mild changes. Signals at lower frequency than NAA (between 1.0 and 1.7 ppm), referred to as "lipids," in spectra located inside the brain were identified in only 3 patients (Patients 2, 13, 14). In these patients the technical quality of the examination was impaired by movement artifacts and we consider it likely that these lipid signals originated from the scalp rather than the brain.

Results

MRI and MRSI Findings

The MRI findings ranged from normal to extensive demyelination in different brain regions, including atrophy in some patients. The MRI findings for the different phenotypes conform to those described previously [20–24]. Comparison of MRSI and MRI results is of particular interest (see Table 1). The MRI was

normal in 5 patients who showed metabolic changes on MRSI. In 8 patients the extent of the signal hyperintensities seen by MRI was smaller than the metabolically changed areas, and in 11 patients the MRI and MRSI findings were equivalent. A normal MRSI combined with an abnormal MRI was observed only in Patient 25, a 70-year-old woman heterozygous for ALD with only mild MRI changes.

Table 2 shows the results of MRSI examinations in ALD patients and control subjects. The NAA/Cho, NAA/Cr, and Cho/Cr ratios are given for spectra in specified locations. White matter was designated as "affected" when there were signal hyperintensities on T2-weighted MRIs, and "unaffected" when white matter appeared normal on MRI. Although two slices were evaluated for each patient and control subject, in some patients alterations were noted in only one slice or only in either occipital or frontal white matter. Results were compared to the mean metabolite ratios in 12 healthy age-matched control subjects. Figure 1 shows the T2-weighted axial MRI as well as four selected spectra and the NAA and Cho spectroscopic images of a 5-year-old and a 30-year-old control person. NAA varied only slightly throughout the whole brain and there was a slightly higher content of Cho in white matter than in gray matter. The NAA/Cho ratio in frontal white matter was somewhat lower than that in occipital white matter, due to a slightly lower NAA and a slightly higher Cho in frontal regions. As indicated in the spectra, the Cr signal was stable in all locations, and the Lac signal was not detectable in the control subjects.

Phenotype: Childhood and Adult Cerebral Adrenoleukodystrophy

The metabolic changes in these patients included an almost complete loss of NAA and a large increase of Cho in the demylinated areas. The findings in Patient 1, in whom there was also increased Lac in the demyelinated regions, are shown in Figure 2. In regions that appeared normal on MRI, milder but significant alterations, namely a decrease of the NAA signal combined with an increase of the Cho signal, were seen in Patient 1 and also in Patient 3. Figure 2A shows the gradual normalization of the metabolic changes between spectra located in the occipital white matter and the frontal white matter (spectra 1–9). The stable Cr signal in the different locations is also demonstrated. Figure 2C shows this improvement, with a parallel increase of NAA and a decrease of Cho from spectra 1 to 9. Only the frontal spectra 8 and 9 show normal metabolite signals (for normal values, see Table 2). Changes, similar to those in white matter, were found in the gray matter spectra of Patient 1, possibly due to partial volume effects of the white matter. Gray matter spectra of Patient 2 showed a mild decrease of all metabolites. We were unable to evaluate spectra in the unaffected white matter in Patient 2 because of frontal susceptibility artifacts.

Phenotype: Adrenomyeloneuropathy

MRSI of all patients showed normal metabolite signals in the gray matter. In 3 patients (Patients 4, 7, and 8) white matter hyperintensities were seen on T2-weighted MRIs. The corresponding metabolic changes in these regions included a decrease of NAA and/or an increase of Cho. No Lac was detected in these areas. As shown in Figure 3, milder metabolic changes in unaffected white matter were noted in Patient 7 (spectra 1 and 2). Metabolic changes in normal-appearing white matter were also detected in Patients 4, 6, and 8. A reduction of the NAA/Cr ratio in frontal as well as in occipital unaffected white matter was found in Patient 6, and a mild increase in the Cho/Cr ratio was detected in the occipital white matter of Patients 4 and 8. MRI and MRSI both appeared normal in Patient 5.

Phenotype: Asymptomatic

Twelve patients with this phenotype were examined. Whereas MRI findings were completely normal in 7 patients (see Table 1), MRSI revealed normal results in only 4 patients (Patients 9, 13, 16, and 17). Even though Patient 12, who at age 2.5 years was the youngest patient in this study, did not have clinical evidence of neurological involvement, his MRIs showed mild white matter changes in the occipital periventricular region. The corresponding metabolic examinations indicated an elevated content of Cho in these regions. These changes were also noted in the frontal and occipital unaffected white matter of this patient. A Cho increase in regions where MRIs looked normal was also noted in Patients 10 (Fig 4), 11, and 15. The NAA signal in the occipital lobe of Patient 19 was decreased in regions that were either normal or abnormal on MRI, while the frontal white matter appeared relatively normal on both MRI and MRSI. MRIs of Patients 14, 18, and 20 showed white matter changes. Metabolic alterations in these patients were noted only in the affected regions, presenting mainly as a decrease of NAA. The MRSI of Patient 20, however, showed a decreased content of all metabolites in the affected areas, as shown in Figure 5 (spectra 3 and 4).

Phenotype: Heterozygote Women

In only 1 (Patient 21) of the 5 women did MRI show changes typical for ALD (Fig 6), with signal hyperintensities in the periventricular white matter. The spectra in these areas indicated both loss of NAA and increased Cho. The same metabolic changes, but within normal-appearing white matter on MRI, were observed in Patient 22 and were more pronounced in the frontal lobe. Both examinations showed normal results in Patient 23. The T2-weighted MRIs of Patient 24,

Table 2. Metabolite Ratios in 25 Patients with Adrenoleukodystrophy and in Different Phenotypes

	Gray Matter			Frontal White Matter Affected			Frontal White Matter Unaffected			Occipital White Matter Affected			Occipital White Matter Unaffected		
	NAA/Cho	NAA/Cr	Cho/Cr	NAA/Cho	NAA/Cr	Cho/Cr	NAA/Cho	NAA/Cr	Cho/Cr	NAA/Cho	NAA/Cr	Cho/Cr	NAA/Cho	NAA/Cr	Cho/Cr
Patient No.[a]															
1	1.17	1.52	1.30				1.17	1.63	1.39	0.30	0.80	2.68			
	1.08	1.47	1.36				1.12	2.39	2.13	0.45	1.70	3.75			
2	2.97	1.57	0.53				ND	ND	ND	0.34	0.76	2.26			
3	2.36	2.04	0.66				1.56	2.00	1.28	0.86	1.72	2.01	1.77	2.03	1.14
	1.77	1.90	1.07				1.43	2.90	2.02	0.72	1.27	1.76			
4	2.15	2.63	1.23	1.18	1.75	1.49				1.21	2.42	2.00	1.42	2.68	1.89
5	2.23	2.15	0.96				2.27	2.96	1.31				1.78	2.25	1.27
6	2.05	1.86	0.91				1.40	1.58	1.13				1.24	2.06	1.66
							1.31	1.88	1.44				1.22	2.00	1.64
7	2.07	2.05	0.99				1.56	2.18	1.40	1.07	1.85	1.73	1.05	2.56	2.44
	2.95	2.37	0.80				1.08	1.62	1.69	0.92	2.00	2.17	1.05	2.47	2.35
8	1.55	2.09	1.35	ND	ND	ND	1.56	2.30	1.48	1.66	3.78	2.28	1.32	2.23	1.69
	2.16	[c]	[c]	1.15	2.45	2.13	1.56	2.36	1.51	ND	ND	ND	1.05	2.65	1.92
9	2.41	2.69	1.12				1.89	2.89	1.53				2.24	2.70	1.21
	2.71	2.53	0.93				2.19	2.46	1.13				2.34	2.66	1.14
10	2.01	[c]	[c]				1.06	2.70	2.53				1.02	2.99	2.94
	2.36	2.06	0.87				1.25	2.56	2.04				1.41	2.46	1.74
11	2.14	2.21	1.03				1.28	2.48	1.93				1.73	2.93	1.70
	2.66	2.27	0.85				1.13	2.94	2.60				1.89	2.69	1.43
12	1.77	2.24	1.26				0.84	2.20	2.63	1.24	[c]	[c]	1.93	2.89	1.50
	1.76	2.92	1.65				1.28	2.12	1.66	1.13	2.74	2.43	1.58	3.17	2.01
13	2.00	2.58	1.29				1.43	3.52	2.45				1.94	2.88	1.48
14	2.27	1.65	0.82				1.55	[c]	[c]	1.30	1.83	1.41	1.81	1.91	1.05
	1.91	2.14	1.12				1.64	[c]	[c]	1.12	1.93	1.72	ND	ND	ND
15	1.88	1.68	1.00				1.26	2.86	2.27				2.13	2.59	1.22
	1.76	[c]	[c]				1.32	2.74	2.07				1.26	2.87	2.29
16	1.71	2.62	1.53				1.43	2.25	1.57				1.81	3.10	1.71
							1.49	2.49	1.67				1.76	2.97	1.68
17	2.02	2.64	1.31				2.29	[c]	[c]				ND	ND	ND
							2.02	2.64	1.31				ND	ND	ND
18	2.34	2.30	0.98				1.81	2.17	1.20	0.15	0.32	2.06			
	ND	ND	ND				1.60	1.91	1.20	0.38	0.86	2.33			
19	1.82	2.15	1.19				1.42	2.84	2.00	0.86	1.22	1.39	1.27	1.94	1.53
	2.42	2.09	0.87				1.33	2.43	1.83				1.95	2.16	1.11
20	2.25	1.97	0.88				1.65	2.21	1.34	0.82	1.37	1.67	2.17	2.40	1.10
	3.29	2.73	0.83				1.56	2.27	1.45	1.81	2.07	1.14	1.95	2.55	1.31
21	1.89	2.45	1.30	1.18	2.24	1.89	1.65	1.52	0.92	0.67	1.40	2.08			
	1.95	1.61	0.94	0.75	1.60	2.13	1.12	2.09	1.87	1.00	1.57	1.57			
22	1.95	1.61	0.93				0.65	1.72	2.02				1.15	1.94	1.69
							1.16	1.69	1.46						
23	1.96	1.80	0.92				1.26	2.31	1.84				1.62	2.78	1.72
	2.19	2.25	1.03				1.40	2.44	1.74				1.52	2.05	1.35
24	2.13	2.71	1.27				1.97	1.58	0.60				3.29	2.49	0.76
	2.00	1.90	0.95				2.33	1.58	0.68				1.91	2.09	1.09
25	3.21	2.88	0.90				1.63	1.98	1.22				1.64	2.05	1.11
	2.60	2.40	0.92				1.54	2.06	1.34				2.29	2.48	1.06
Controls	2.15	2.20	1.05				1.71	2.61	1.55				1.91	2.82	1.49
STD	0.48	0.41	0.23				0.26	0.50	0.31				0.36	0.58	0.24
Phenotype[b]															
cALD															
Mean	1.67	1.70	1.02				1.32	2.23	1.70	0.53	1.25	2.49	1.77	2.03	1.14
Min	1.08	1.47	0.53				1.12	1.63	1.28	0.30	0.76	1.76	1.77	2.03	1.14
Max	2.97	2.04	1.36				1.56	2.90	2.13	0.86	1.72	3.75	1.77	2.03	1.14
AMN															
Mean	2.17	2.19	1.04	1.16	2.10	1.81	1.53	2.16	1.42	1.21	2.51	2.05	1.27	2.36	1.86
Min	1.55	1.66	0.80	1.15	1.75	1.49	1.08	1.58	1.13	0.92	1.85	1.73	1.05	2.00	1.27
Max	2.95	2.63	1.35	1.18	2.45	2.13	2.27	2.96	1.69	1.66	3.78	2.28	1.78	2.68	2.44
Asymptomatic															
Mean	2.17	2.33	1.09				1.51	2.54	1.82	0.98	1.54	1.77	1.79	2.66	1.56
Min	1.71	1.85	0.62				0.64	1.91	1.13	0.15	0.32	1.14	1.02	1.91	1.05
Max	3.29	2.92	1.65				2.29	3.52	2.63	1.61	2.74	2.43	2.34	3.17	2.94
Heterozygote															
Mean	2.21	2.22	1.02	0.97	1.92	2.01	1.49	1.90	1.39	0.84	1.48	1.62	1.95	2.27	1.26
Min	1.69	1.80	0.90	0.75	1.60	1.69	0.85	1.52	0.68	0.67	1.40	1.57	1.15	1.94	0.76
Max	3.21	2.88	1.30	1.18	2.24	2.13	2.33	2.44	2.02	1.00	1.57	2.08	3.29	2.78	1.72
Controls															
Mean	2.15	2.20	1.05				1.71	2.61	1.55				1.91	2.82	1.49
STD	0.48	0.41	0.23				0.26	0.50	0.31				0.36	0.59	0.24

[a]The NAA/Cho, NAA/Cr, and Cho/Cr ratios in spectra located in gray matter, frontal white matter, and occipital white matter are compared to the mean values of 12 healthy control subjects (STD = standard deviation). The frontal and occipital regions of the white matter are further divided into affected and unaffected (see text).

[b]The mean values and ranges (Min = minimum value; Max = maximum value; STD = standard deviation) of metabolite ratios in spectra located in the designated regions for the different phenotypes are compared to the mean values of 12 healthy control subjects.

[c]Values not reliably interpretable because of the influence of a relatively high Cho signal impairing the Cr signal.

ND = not determined due to poor spectral quality; NAA = *N*-acetyl aspartate; Cho = choline-containing compounds; Cr = creatine and phosphocreatine; cALD = childhood adrenoleukodystrophy; AMN = adrenomyeloneuropathy.

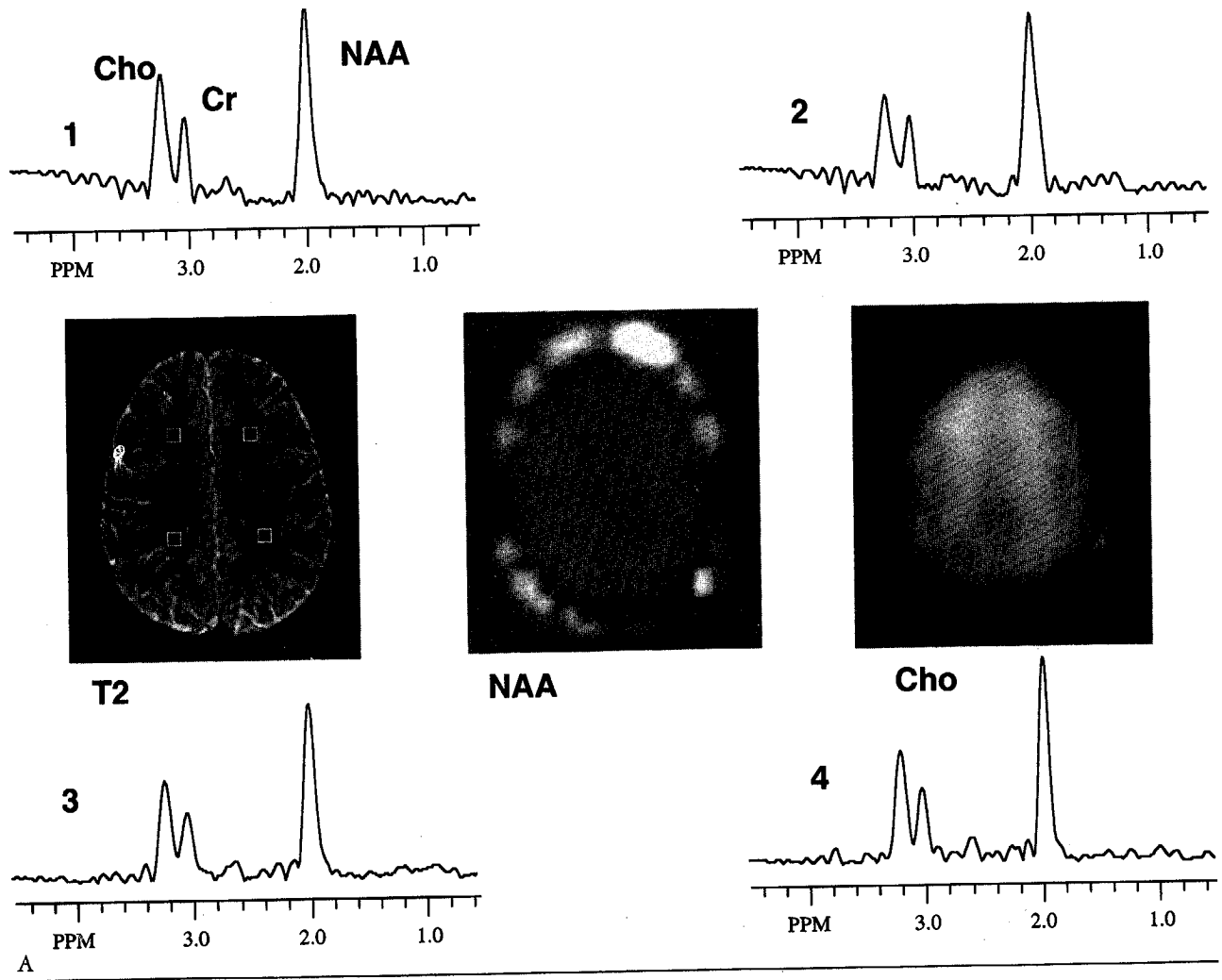

Fig 1. T2-weighted axial magnetic resonance image of a 5-year-old (A) and a 30-year-old (B) healthy control person with voxels located in frontal and parietooccipital white matter, respectively. Corresponding locations of the spectra were chosen in all patients. The spectra show normal metabolite ratios and the N-*acetyl aspartate* (NAA) *and choline-containing compound* (Cho) *spectroscopic images show the usual contrast for gray and white matter. In the NAA images the bright spots surrounding the brain originate from skull lipids, which are in the same chemical shift range. Cr = creatine and phosphocreatine.*

who is the 70-year-old twin of Patient 25, showed signal hyperintensities in the basal ganglia and cerebellar peduncles. We are not certain that these alterations are attributable to ALD. Metabolic changes, namely a loss of all metabolites, were noted not only in these areas but also in periventricular frontal and occipital white matter. T2-weighted images of Patient 25 showed signal hyperintensities in the pons combined with a mild cerebellar atrophy below where the MRSI bottom slice was made. Metabolic patterns were normal in all regions examined by MRSI. The gray matter spectra appeared normal in all 5 patients.

Statistical Considerations

Table 2 compares the MRSI findings in individual patients and control subjects and demonstrates that the findings differed from normal by more than 2 standard deviations in at least one voxel in 18 of these patients. Since the MRSI was normal in 7 of the ALD patients and the patient numbers in the phenotype groups were small, the difference from normal for the ALD group as a whole, or for the various phenotype groups, did not reach statistical significance.

We also carried out a statistical analysis of the data in the last two columns of Table 1. In 5 of the 25 patients, MRSI was abnormal when MRI was normal. There was only 1 patient for whom MRI was abnormal when MRSI was normal, namely Patient 25, a 70-year-old woman who was heterozygous for ALD. While in this last patient the MRI abnormalities may have been unrelated to ALD, we nevertheless included this result

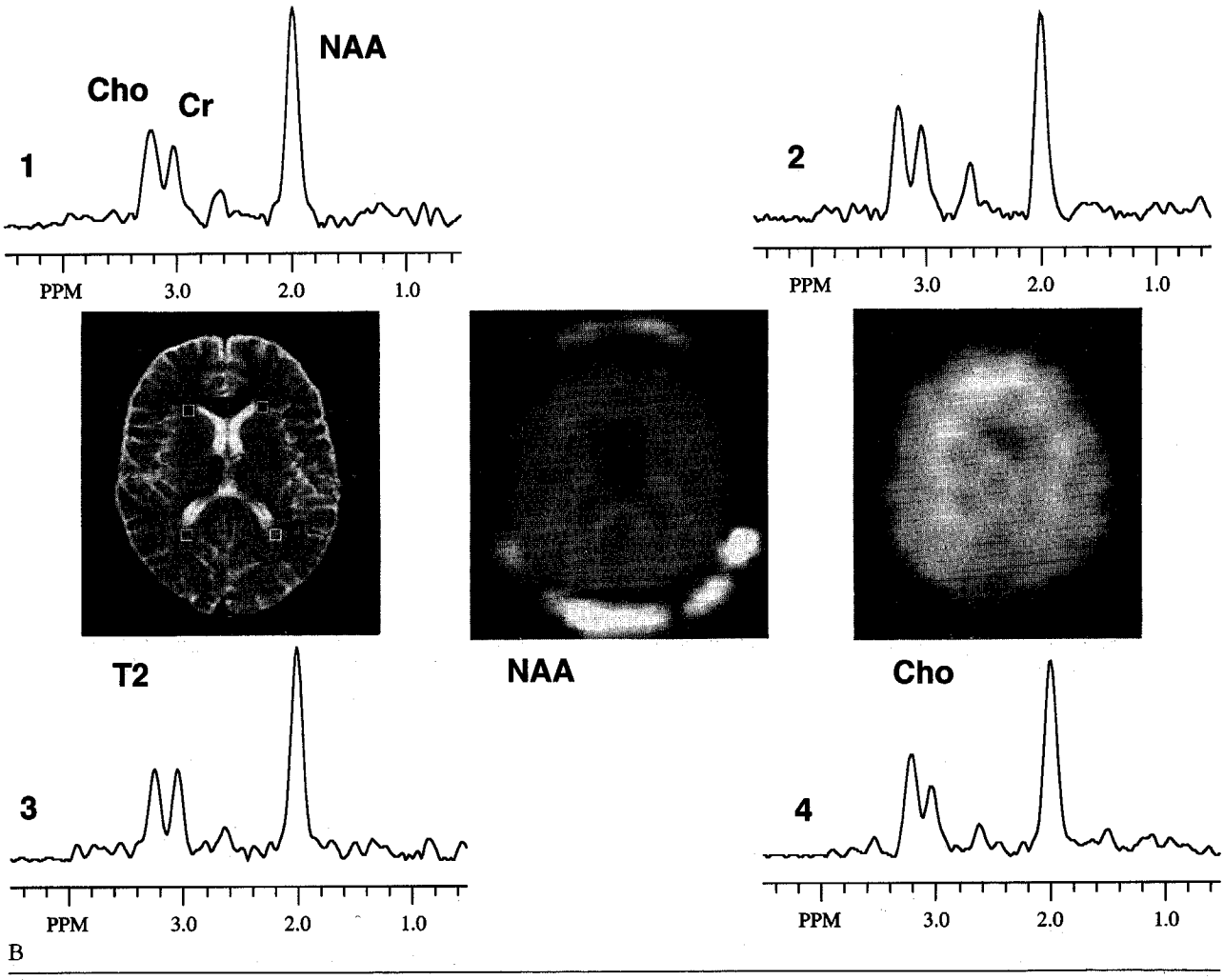

in our analysis. In order to exclude bias as much as possible, for the purpose of this calculation, we also classified as "equivalent abnormal" the 8 patients in whom the MRSI was considered to show a greater degree of abnormality than the MRI, since this comparison may include a judgmental factor that is difficult to quantify. However, even when we restrict the statistical analysis to the 6 patients in whom the contrast between MRI and MRSI was normal versus abnormal, MRSI was found to show a significantly higher incidence of abnormal findings than MRI, with a p value of 0.009 (χ^2 test). It is important to emphasize that this finding indicates only that MRSI findings are more frequently abnormal than are MRI results. The clinical significance of this finding is not yet clear. While it is our working hypothesis that patients in whom MRSI and MRI results are both normal are less likely to develop clinically evident cerebral involvement than are patients in whom results of one or both of these studies are abnormal, longer follow-up is needed to determine if this is indeed the case.

Discussion

The current study demonstrates the feasibility of performing multislice proton spectroscopic imaging, together with conventional MRI, in control subjects and ALD patients. Good-quality spectroscopic images were obtained from all examinations. However, interpretation of MRSI data sets requires care; for instance, it was often observed that the lowest (most inferior) slice showed drop-off signal intensity in the most anterior brain regions. This arose from poor magnetic field homogeneity in these regions, rather than from a decrease in metabolite levels. This can readily be determined by inspecting spectra from these regions. In other images, it is also possible to see the octagonal profile of the outer volume saturation pulses in regions close to the skull (e.g., the NAA and Cho images in Fig 4). Finally, it should be kept in mind that spectroscopic images may contain artifacts from residual water and lipid signals; for instance, the NAA image in Figure 1A shows lipid contamination from the pericranial fat, particularly in the left anterior region. Also, in Figure

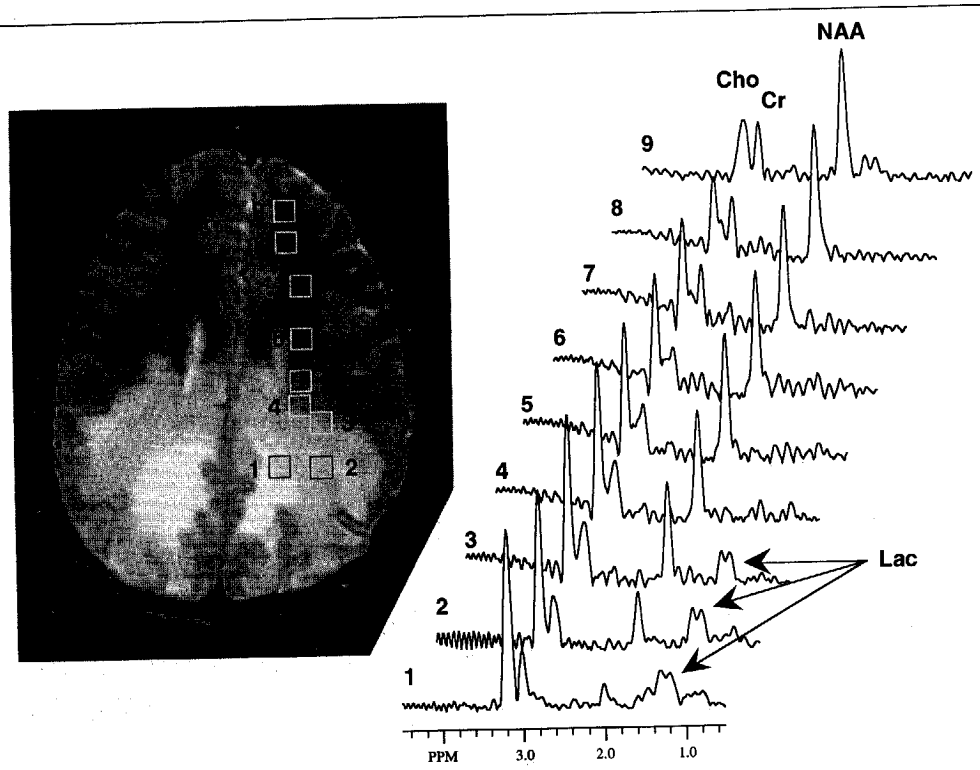

A

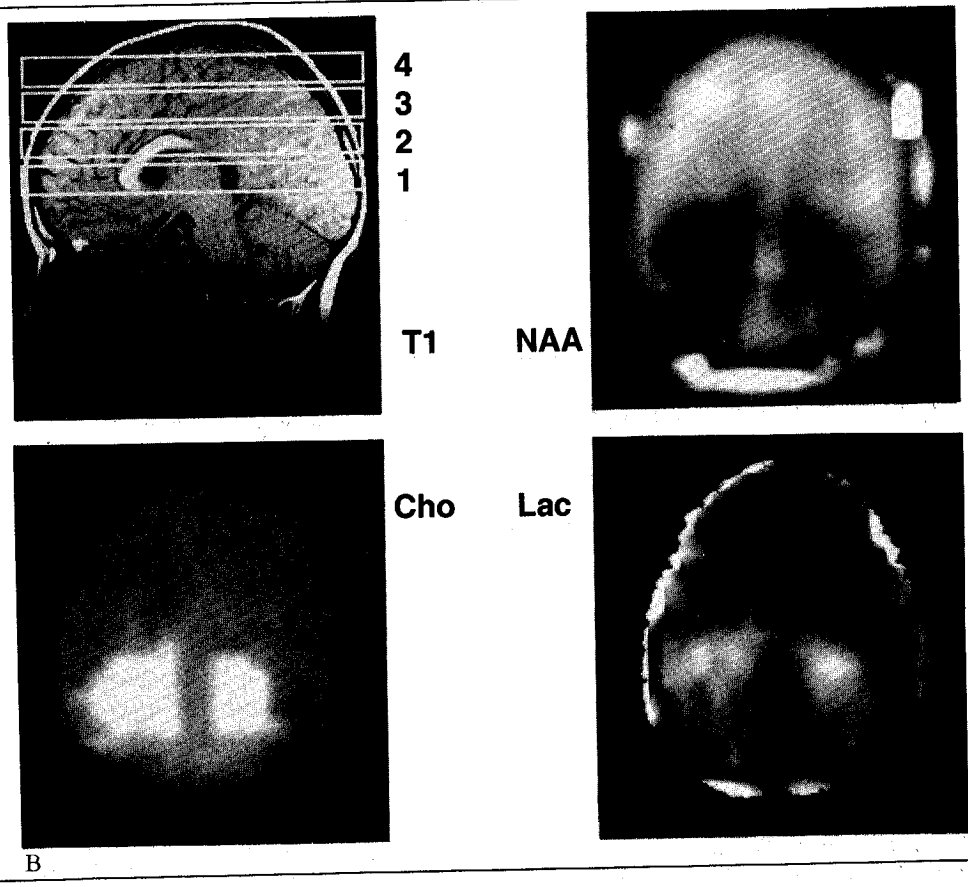

B

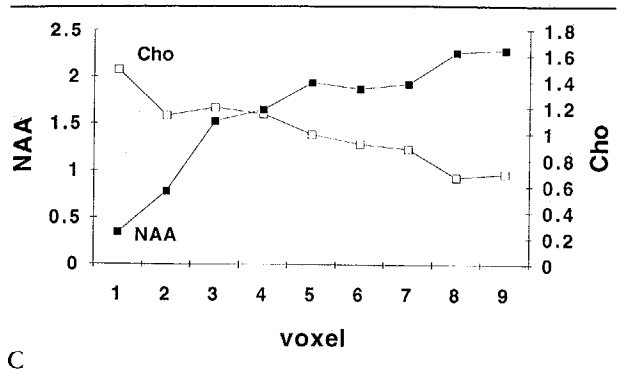

C

Fig 2. Patient 1 (childhood cerebral-type adrenoleukodystrophy). (A) T2-weighted magnetic resonance image (MRI) with the location of nine selected voxels. The signal hyperintensities in the occipitoparietal white matter indicate demyelinated areas. The spectra referring to the indicated voxels are shown on the right. Voxels 1 and 2 are located in the center and 3 and 4 at the edge of the demyelinated area; voxels 5 through 9 are placed in normal-appearing white matter. (B) T1-weighted sagittal MRI indicating the four slices used for magnetic resonance spectroscopic imaging (MRSI). N-acetyl aspartate (NAA), *choline-containing compounds* (Cho), *and lactate* (Lac) *spectroscopic images of slice 3 with a decrease of NAA (hypointense areas in the occipital lobe) and increases of Cho and Lac (hyperintensities) are shown. NAA and Lac images show the usual bright lipid ring around the brain. (C) Amounts of NAA and Cho in nine selected voxels, given as integrals of the peak areas as measured by MRSI. Note the nearly complete loss of NAA, the large increase of Cho, and the moderate increase of Lac in the demyelinated area. These metabolic changes improve gradually with the increasing distance from the demyelinated zone, but even in normal-appearing white matter (voxels 5–7) metabolic changes (NAA decreases and Cho increases) are present. Only the spectra in the very frontal white matter (8, 9) appear normal. The creatine and phosphocreatine* (Cr) *signal is relatively stable in all voxels.*

5, the Cho image shows some signal intensity in the ventricle; this arises from residual water (not choline) which is less efficiently suppressed in cerebrospinal fluid. All of these effects may be readily appreciated by examining the spectra from each of these regions.

Metabolic Alterations

An increase of Cho and a decrease of the NAA signal were the most striking MRSI abnormalities in ALD patients and were observed to various degrees with all phenotypes. These changes were reported previously by us and others [25–27] using single-voxel spectroscopy. Our findings in asymptomatic patients are also in agreement with the previous reports of Tzika and colleagues [28, 29], which demonstrated that affected white matter showed total choline to be significantly higher in ALD versus control subjects. Also in other white matter disorders, such as metachromatic leukodystrophy [30], multiple sclerosis [31, 32], and acquired immunodeficiency syndrome (AIDS) [33], an increase of Cho and a decrease of the NAA signal have been detected.

Since NAA has been reported to be a neuronal component exclusively [34], we cannot explain why it is reduced even in early ALD white matter lesions, since loss of myelin is the predominant abnormality in ALD. It may reflect the loss of oligodendrocytes or neuroaxonal abnormalities that occur as the disease advances [35]. The physiological role of NAA is not completely understood. Besides its role as an anion, it may serve as a source of acetyl groups for lipid synthesis and myelination [36]. Recent reports of a reduction of NAA in white matter of patients with diabetes mellitus [37], and the confirmation of these findings in animal studies [38], suggest that NAA might also be decreased because of a metabolic rather than a structural neuroaxonal defect in demyelinating lesions [39].

Cho compounds are constituents of cell membranes. They were found to be elevated in the brains of many ALD patients. Demyelinative processes might induce increased membrane turnover and therefore elevate the free Cho content. Magnetic resonance spectroscopy studies of perchloric acid extracts of dog brain demonstrated that about 80% of the Cho resonance can be attributed to glycerophosphocholine and phosphocholine, both membrane precursors and/or degradation products (P. B. Barker et al., unpublished data, 1994). The detection of increased Cho by MRSI not only in demyelinated regions but also in unaffected white matter might be the first sign of onset of demyelination, not yet detectable as a signal hyperintensity on MRI. Biochemical studies of brain in ALD patients showed an increased content of VLCFAs predominantly in phosphatidylcholine [40], a major component of cell membranes. It was concluded that this chemical alteration of the membrane lipids might be a triggering process for demyelination. Whether, and to what extent, phosphatidylcholine contributes to the Cho signal detected by MRSI in ALD patients (and control subjects) remain unclear.

MRSI detected Lac in the center as well as at the edge of the demyelinated region only in Patient 1 (cALD). This metabolite was not detected in patients with other phenotypes, even in affected white matter. Magnetic resonance spectroscopy also revealed elevated Lac activity in severely damaged regions of brains in patients with other leukodystrophies, probably due to infiltrated macrophages [30]. Macrophages are present in demyelinated regions in cALD and aALD patients with active inflammatory responses [1]. Therefore the presence of Lac may be due to active inflammation or severe tissue damage causing impaired blood perfusion and resulting ischemia.

The normal MRSI findings in gray matter are consis-

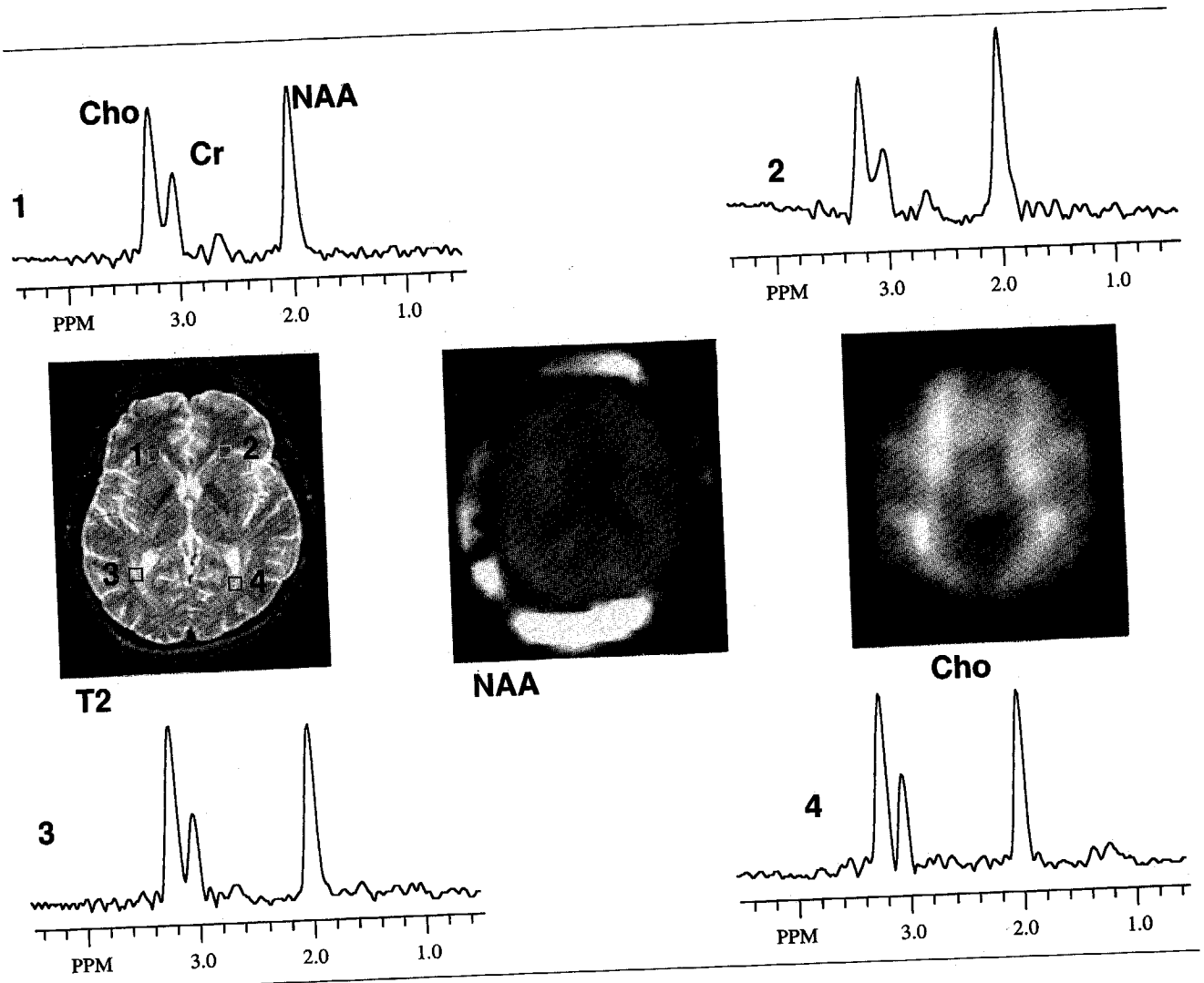

Fig 3. Patient 7 (adrenomyeloneuropathy). T2-weighted axial magnetic resonance imaging with four selected voxels in periventricular normal-looking frontal white matter (voxels 1 and 2) and in affected periventricular occipital white matter (voxels 3 and 4). The corresponding spectra and the N*-acetyl aspartate* (NAA) *and choline-containing compounds* (Cho) *spectroscopic images indicate metabolic changes (NAA decreases and Cho increases) not only in affected but also in unaffected white matter. Cr = creatine and phosphocreatine.*

tent with the lack of neuronal abnormalities in autopsy studies in this tissue.

Clinical Value of MRSI Examinations

Correlation of MRSI with clinical and MRI findings indicates that MRSI can provide new information that is critical for prognosis, counseling, and management decisions. In 50% of the ALD patients examined, MRSI demonstrated a greater capacity to detect brain abnormalities than did MRI. Consequently, it can aid our ability to distinguish patients who have very early brain involvement from those who have none, a distinction that, as already noted, has important implications for management decisions. Nevertheless, the prognostic significance of mild MRI abnormalities, and even more important, of mild MRSI abnormalities, is not yet understood. Neurologically asymptomatic ALD patients with mild MRI changes may remain clinically stable without further progression of the MRI abnormalities for more than 4 years (e.g., Patient 20) [41], while in others the neurological and MRI abnormalities do advance. Further follow-up is required to define the natural history and effects of therapeutic interventions. We anticipate that the addition of the highly sensitive MRSI to the standard MRI will enhance our capacity to distinguish stable abnormalities from those that are progressive.

Our findings also suggest that the height of the Cho peak may correlate with the degree of activity of the demyelinating process in regions of brain where the MRI already demonstrates abnormality. Elevated Cho

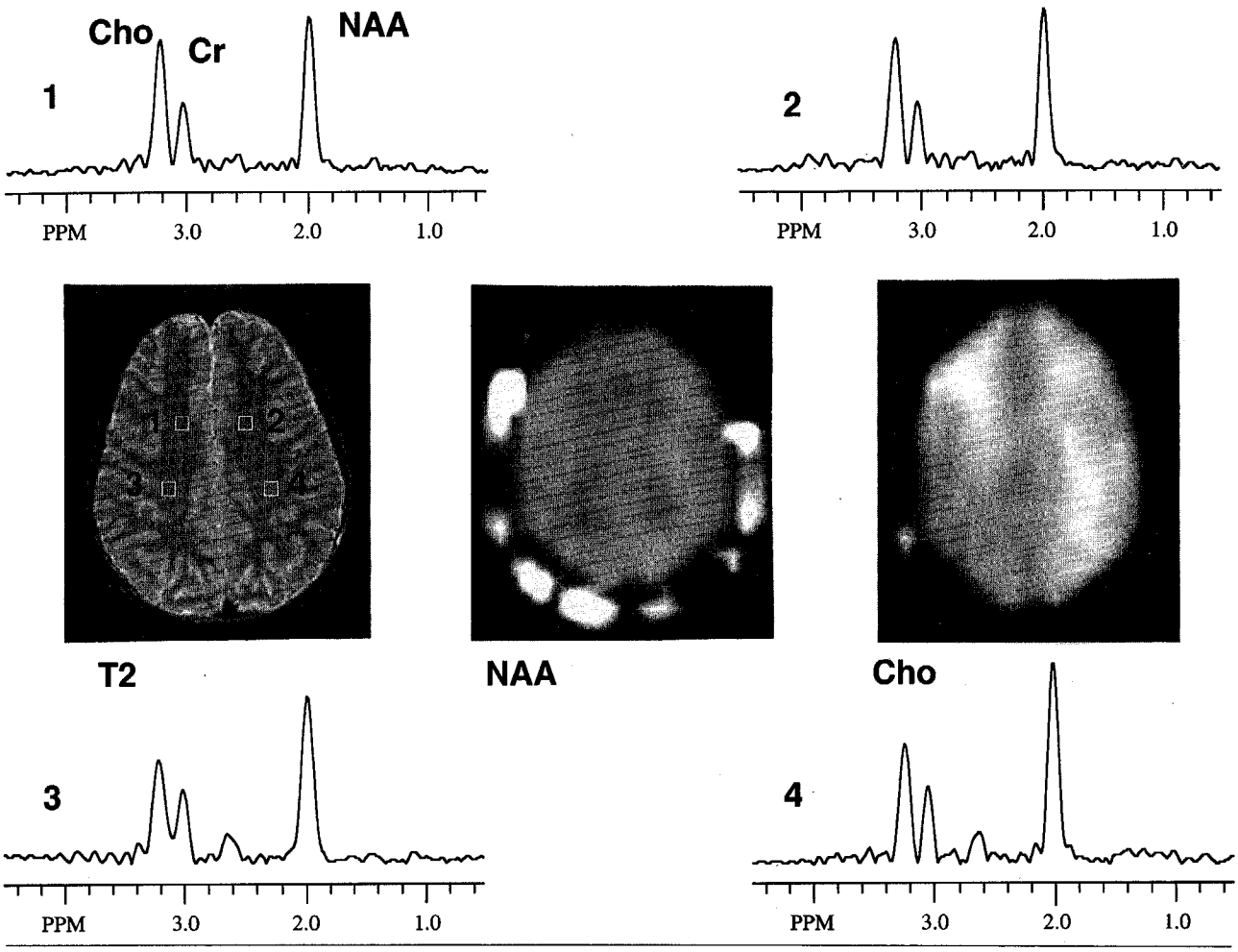

Fig 4. Patient 10 (asymptomatic). T2-weighted axial magnetic resonance imaging (MRI) with location of four voxels, the corresponding spectra, and the N-*acetyl aspartate* (NAA) *and choline-containing compound* (Cho) *spectroscopic images. Whereas the MRI fails to show obvious white matter changes, a decrease of NAA and a mild increase of Cho in bilateral frontal white matter are indicated in the spectra and in the spectroscopic images. Cr = creatine and phosphocreatine.*

peaks were noted in Patients 1, 3, 7, and 21, whose neurological disability was increasing rapidly. This contrasted with the finding in Patient 20, whose clinical status and MRI abnormality had remained static for the previous 4 years. In this patient, all metabolites, including Cho, were reduced in the regions in which the MRI appearance was abnormal. Corresponding findings have also been made in 2 patients examined by use of short-echo-time, single-voxel, localized proton magnetic resonance spectroscopy (J. Frahm, personal communication, 1993).

The finding of increased Cho without a change in the NAA signal in asymptomatic Patients 10, 11, 12, and 15 indicates that this might be the first recognizable metabolic alteration and may reflect the onset of demyelination without neuroaxonal damage.

It has been hypothesized that the pathogenetic mechanism of the rapidly progressive childhood, adolescent, and adult cerebral forms of ALD differ from the mechanisms in patients with the slowly progressive AMN and the other phenotypes that are milder [9, 42]. The rapidly progressive cerebral forms are characterized by an inflammatory response that is associated with increased levels of cytokines such as tumor necrosis factor-α [42], or autoimmune mechanisms [43], which are absent or less pronounced in the milder phenotypes. In the regions showing an active inflammatory response there is also disruption of the blood-brain barrier [8], which can be demonstrated with contrast medium on MRI. The combined use of contrast-enhanced MRI and MRSI should offer the possibility of assessing the degree of both the inflammatory response in the brain and the activity of the demyelina-

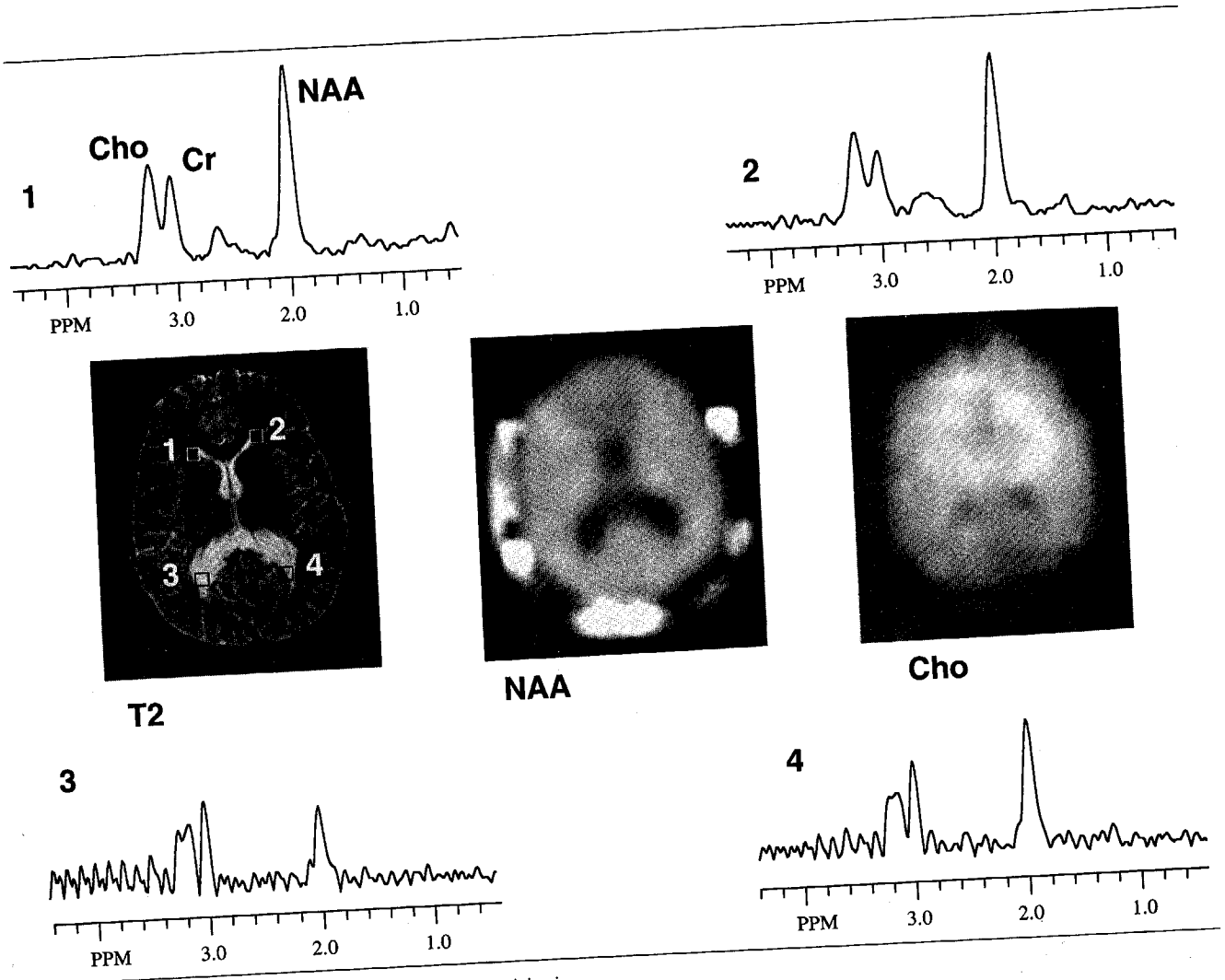

Fig 5. Patient 20 (asymptomatic). Signal hyperintensities in the occipital periventricular white matter concomitant with metabolic changes in this region (voxels 3 and 4) compared to the normal-appearing frontal white matter (voxels 1 and 2) can be noted in the T2-weighted magentic resonance image and spectra of the indicated voxels. The low signal-noise ratio in both voxels located in the affected white matter indicates a decrease of all metabolites in this region. The N-*acetyl aspartate* (NAA) *and choline-containing compounds* (Cho) *spectroscopic images demonstrate the normal distribution of these metabolites in this slice except for in the occipital periventricular white matter. Cr = creatine and phosphocreatine.*

tive process, and of improving our capacity to evaluate the indications and effectiveness of therapeutic interventions.

In conclusion, the initial findings of our ongoing study establish the high sensitivity of a multislice MRSI technique for determination of central nervous system involvement in ALD patients, in particular, for demonstrating metabolic alterations in structurally unaffected white matter. The earliest alteration in asymptomatic patients is an increase in the Cho signal. In later stages of the disease there is an additional decrease in NAA, which may be followed by an increase in Lac. Comparison of MRSI results with the clinical course suggests that the nature of the metabolic alterations can serve as an indicator for disease activity.

Parts of this work were presented at the 12th Annual Meeting of the Society of Magnetic Resonance in Medicine, New York, NY, Aug 1993, and at the Annual Meeting of the Childhood Neurology Society, Lake Buena Vista, FL, Oct 1993.

Financial support was given by grants HD 10981, RR 00035, RR 00052, and RR 00722 from the National Institutes of Health, grant FD-R-000685 from the Food and Drug Administration, and grant Kr 1337/1-1 from the Deutsche Forschungsgemeinschaft (to B. K.).

We are grateful to Joe Gillen, PhD, and Jeff Sobering, PhD, for their work on the development of the MRSI method and to the staff members of the Kennedy Krieger Institute and the Department of Radiology, Johns Hopkins Medical School, for their help in organizing the examinations. We also thank Pamela Talalay, PhD, for helpful advice and Jan Shankroff, MS, for performing the statistical analysis.

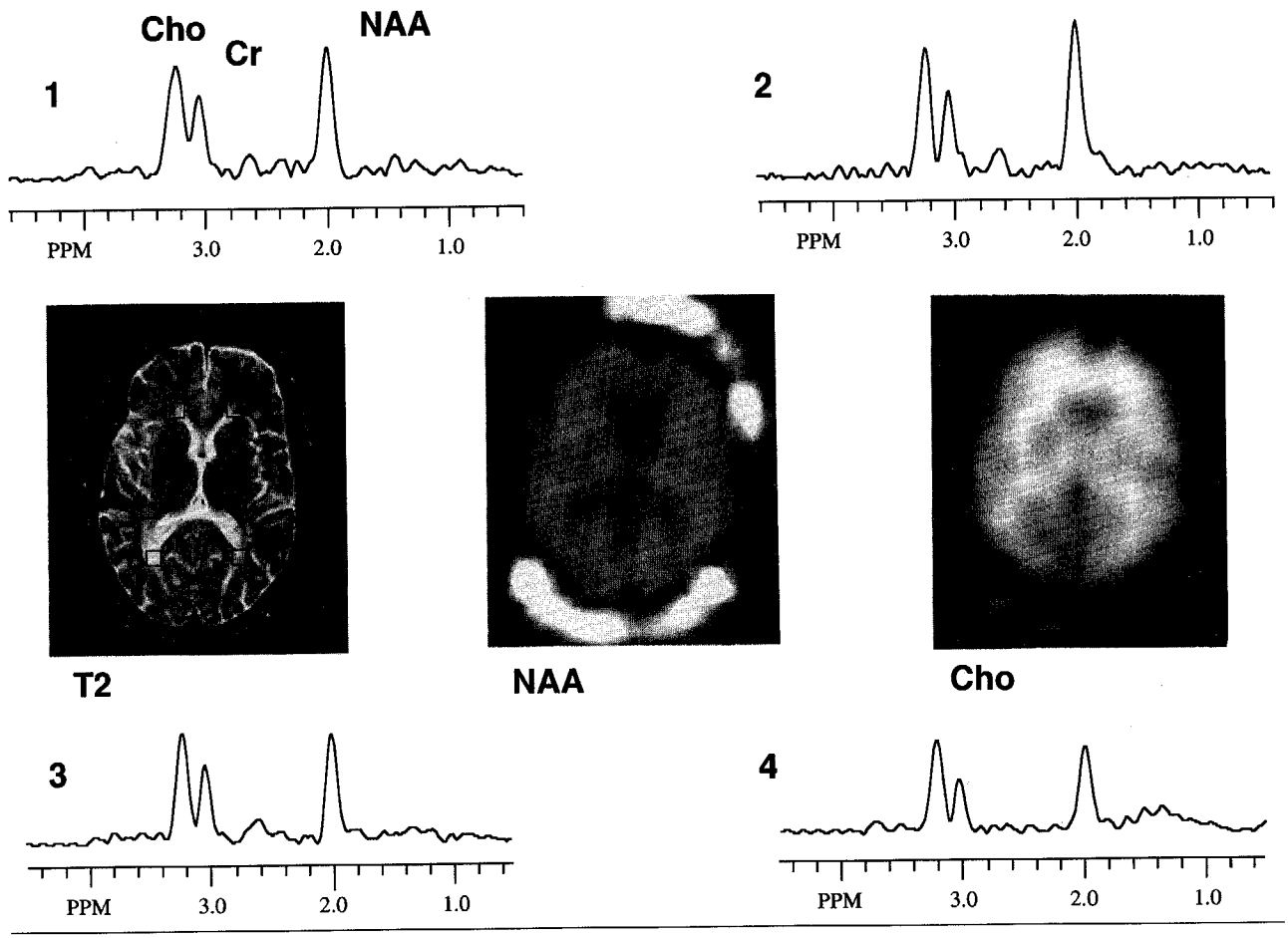

Fig 6. Patient 21 (heterozygote). T2-weighted axial magnetic resonance image showing signal hyperintensities in frontal and occipital periventricular regions of white matter with the location of four selected voxels. The corresponding spectra show metabolic changes appearing as a decrease of N-*acetyl aspartate* (NAA) *and a milder increase of choline-containing compounds* (Cho) *in all selected voxels. This is also demonstrated in the NAA and Cho spectroscopic images. Cr = creatine and phosphocreatine.*

References

1. Moser HW, Moser AB. Adrenoleukodystrophy (X-Linked). In: Scriver CR, Beaudet AL, Sly WS, Valle D, eds. The metabolic basis of inherited disease. New York: McGraw-Hill, 1989: 1511–1532
2. Igarashi M, Schaumburg HH, Powers JM, et al. Fatty acid abnormality in adrenoleukodystrophy. J Neurochem 1976;26: 851–860
3. Moser HW, Moser AB, Frayer KK, et al. Adrenoleukodystrophy: increased plasma content of saturated very long chain fatty acids. Neurology 1981;31:1241–1249
4. Tsuji S, Suzuki M, Ariga T, et al. Abnormality of long-chain fatty acids in erythrocyte membrane sphingomyelin from patients with adrenoleukodystrophy. J Neurochem 1981;36: 1046–1049
5. Lazo O, Contreras M, Hashmi M, et al. Peroxisomal lignoceroyl-CoA ligase deficiency in childhood adrenoleukodystrophy and adrenomyeloneuropathy. Proc Natl Acad Sci USA 1988;85: 7647–7651
6. Migeon BR, Moser HW, Moser AB, et al. Adrenoleukodystrophy: evidence for X-linkage, inactivation and selection favoring the mutant allele in heterozygous cells. Proc Natl Acad Sci USA 1981;78:5066–5070
7. Mosser J, Douar AM, Sarde CO, et al. Putative X-linked adrenoleukodystrophy gene shares unexpected homology with ABC transporters. Nature 1993;361:726–730
8. Schaumburg HH, Powers JM, Raine CS, et al. Adrenoleukodystrophy: a clinical and pathology study of 17 cases. Arch Neurol 1975;33:577–591
9. Moser HW, Moser AB, Smith KD, et al. Adrenoleukodystrophy: phenotypic variability and implications for therapy. J Inherit Metab Dis 1992;15:645–664
10. Griffin JW, Goren E, Schaumburg H, et al. Adrenomyeloneuropathy: a probable variant of adrenoleukodystrophy. Neurology 1977;27:1107–1113
11. Moser HW, Moser AB, Naidu S, Bergin A. Clinical aspects of adrenoleukodystrophy and adrenomyeloneuropathy. Dev Neurosci 1991;13:254–261
12. Aubourg P, Blanche S, Jambaque I, et al. Reversal of early neurologic and neuroradiologic manifestations of X-linked adrenoleukodystrophy by bone marrow transplantation. N Engl J Med 1990;322:1860–1866

13. Moser HW, Tutschka PJ, Brown FR III, et al. Bone marrow transplant in adrenoleukodystrophy. Neurology 1984;34:1410–1417
14. Shapiro EG, Klein KA. Dementia in childhood: issues in neuropsychological assessment with application to the natural history and treatment of degenerative storage diseases. In: Tramontana MG, Hooer SR, eds. Advances in child neuropsychology. New York: Springer, 1993:119–171
15. Duyn JH, Gillen J, Sobering G, et al. Multisection proton MR spectroscopic imaging of the brain. Radiology 1993;18:277–282
16. Moonen CTW, Sobering G, van Zijl PCM, et al. Proton spectroscopic imaging of human brain. J Magn Reson 1992;98:556–575
17. Moonen CTW, van Zijl PCM. Highly effective water suppression for in vivo proton NMR spectroscopy. J Magn Reson 1990; 88:28–41
18. Michaelis T, Merboldt KD, Bruhn H, et al. Absolute concentrations of metabolites in the adult human brain in vivo: quantification of localized proton MR spectra. Radiology 1993;187:219–227
19. Barker PB, Soher BJ, Blackband SJ, et al. Quantitation of proton NMR spectra of the human brain using tissue water as an internal concentration reference. NMR Biomed 1993;6:89–94
20. Kumar AJ, Rosenbaum AE, Naidu S, et al. Adrenoleukodystrophy: correlating MR imaging with CT. Radiology 1987;165: 496–504
21. Jensen ME, Sawyer RW, Braun IF, Rio WB. MR imaging appearance of childhood adrenoleukodystrophy with auditory, visual, and motor pathway involvement. Radiographics 1990;10: 53–66
22. Aubourg P, Sellier N, Chaussain JL, Kalifa G. MRI detects cerebral involvement in neurologically asymptomatic patients with adrenoleukodystrophy. Neurology 1989;39:1619–1621
23. Aubourg P, Adamsbaum C, Lavallard-Rousseau MC, et al. Brain MRI and electrophysiologic abnormalities in preclinical and clinical adrenomyeloneuropathy. Neurology 1992;42:85–91
24. Loes DJ, Hite S, Moser HW, et al. Adrenoleukodystrophy: development of a scoring method for brain MR observations. AJNR 1994 (in press)
25. Bruhn H, Kruse B, Michaelis T, et al. Morphologic and metabolic alterations in adrenoleukodystrophies. A combined MRI and proton MRS study of CNS involvement in vivo. In: Society of Magnetic Resonance in Medicine, 11th annual meeting, Berlin, Germany. 1992:235 (Abstract)
26. Confort-Gouny S, Vion-Dury J, Chabrol B, et al. Localized proton MR spectroscopy in X-linked adrenoleukodystrophy. In: Society of Magnetic Resonance in Medicine, 12th annual meeting, New York, NY. 1993:1565 (Abstract)
27. Grad J, Stillman AE, Krivit W, et al. Proton magnetic resonance spectroscopy in patients with adrenoleukodystrophy. In: Society of Magnetic Resonance in Medicine, 12th annual meeting, New York, NY. 1993:283 (Abstract)
28. Tzika AA, Ball WS, Vigneron DB, et al. Clinical proton MR spectroscopy of neurodegenerative disease in childhood. AJNR 1993;14:1267–1281
29. Tzika AA, Ball WS, Vigneron DB, et al. Childhood adrenoleukodystrophy: assessment with proton MR spectroscopy. Radiology 1993;189:467–480
30. Kruse B, Hanefeld F, Christen HJ, et al. Alterations of brain metabolites in metachromatic leukodystrophy as detected by localized proton magnetic resonance spectroscopy in vivo. J Neurol 1993;241:68–74
31. Bruhn H, Frahm J, Merboldt KD, et al. Multiple sclerosis in children. Cerebral metabolic alterations monitored by localized proton magnetic resonance spectroscopy in vivo. Ann Neurol 1992;34:140–150
32. Arnold DL, Mattews PM, Francis G, et al. Proton magnetic resonance spectroscopy in human brain in vivo in the evaluation of multiple sclerosis: assessment of the load of the disease. Magn Reson Med 1990;14:154–159
33. Vion-Dury J, Confort-Gouny S, Nicoli F, et al. Localized brain proton MRS in neurologic complications of AIDS: value for diagnosis and prognosis. In: Society of Magnetic Resonance in Medicine, 12th annual meeting, New York, NY. 1993:1563 (Abstract)
34. Birken DL, Oldendorf WH. *N*-acetyl-L-aspartic acid: a literature review of a compound prominent in ^{1}H-NMR spectroscopic studies of brain. Neurosci Biobehav Rev 1989;1:23–31
35. Powers JM. Adrenoleukodystrophy (adreno-testiculo-leukomyelo-neuropathic-complex). Clin Neuropathol 1985;4:181–199
36. D'Adamo AF, Yatsu FM. Acetate metabolism in the nervous system. *N*-acetyl-L-aspartic acid and the biosynthesis of brain lipids. J Neurochem 1966;13:961–965
37. Kreis R, Ross BD. Cerebral metabolic disturbances in patients with subacute and chronic diabetes mellitus: detection with proton MR spectroscopy. Radiology 1992;184:123–130
38. Brenner RE, Beech JS, Williams SCR, et al. Reversibility of the reduction of NAA in diabetic ketoacidosis. In: Society of Magnetic Resonance in Medicine, 12th annual meeting, New York, NY. 1993:1559 (Abstract)
39. Brenner RE, Munro PMG, Williams SCR, et al. Abnormal neuronal mitochondria: a cause of reduction in NA in demyelinating disease. In: Society of Magnetic Resonance in Medicine, 12th annual meeting, New York, NY. 1993:281 (Abstract)
40. Sharp P, Johnson D, Poulos A. Molecular species of phosphatidylcholine containing very long chain fatty acids in human brain: enrichment in X-linked adrenoleukodystrophy brain and diseases of peroxisome biogenesis brain. J Neurochem 1991;56: 30–37
41. Moser HW, Kok F, Neumann S, et al. Adrenoleukodystrophy update: genetics and effect of Lorenzo's oil therapy in asymptomatic patients. Int Pediatr 1994 (in press)
42. Powers JM, Liu Y, Moser AB, Moser HW. The inflammatory myelinopathy of adreno-leukodystrophy: cells, effector molecules, and pathogenetic implications. J Neuropathol Exp Neurol 1992;51:630–643
43. Griffin DE, Moser HW, Mendoza Q, et al. Identification of the inflammatory cells in the nervous system of patients with adrenoleukodystrophy. Ann Neurol 1985;18:660–664